

Multifractal Analysis of Thermal Images of Electronic Devices in Different Colour Profiles

Marina Díaz-Jiménez
Dept. Computer Science Eng.
University of Cádiz, Spain
email: marina.diaz@uca.es

Juan Carlos de la Torre
Dept. Computer Science Eng.
University of Cádiz, Spain
email: juan.detorre@uca.es

Javier Jareño-Dorado
Dept. Computer Science Eng.
University of Cádiz, Spain
email: javier.jareno@uca.es

Patricia Ruiz
Dept. Mechanical Eng. and Ind. Design
University of Cádiz, Spain
University of Sydney, Australia
email: patricia.ruiz@uca.es

Bernabé Dorronsoro
Dept. Computer Science Eng.
University of Cádiz, Spain
University of Sydney, Australia
email: bernabe.dorronsoro@uca.es

Pablo Pavón-Domínguez
Dept. Mechanical Eng. and Ind. Design
University of Cádiz, Spain
email: pablo.pavon@uca.es

Abstract—Nowadays, there are many methods for analysing images. Among them, a multifractal approach is able to characterise images in terms of the complexity of patterns they contain. However, multifractal methods are very sensitive to small changes in colour images. This study presents a preliminary study for the accurate characterisation of electronic devices in terms of heat dissipation using multifractal analysis. Specifically, a novel methodology using multifractal approach is proposed to characterise images in different colour formats: Grey-Scale, Red-Green-Blue (RGB), Cyan-Magenta-Yellow-Key (CMYK), Hue-Saturation-Value (HSV) and Hue-Saturation-Intensity (HSI), and the results are compared. For this purpose, thermal images of a Pi3 Raspbian Desktop board are analysed with the aim of finding out the results of the multifractal analysis on different areas of the board. Multifractal analysis is carried out through the box-counting method and the method of moments, since they allow to extract the main multifractal parameters, such as, the generalised dimensions function, $D(q)$ and the degree of multifractality, $\Delta D(q)$. The results obtained show that both scaling properties and multifractal parameters vary according to the colour format, i.e., the same image exhibits different multifractal properties depending on the colour format.

Keywords - Multifractal analysis; thermal images; colour formats; box-counting; colour images.

I. INTRODUCTION

Fractal shapes are mainly characterised by self-similar properties and a fractal dimension (D_f), which is dependent of the scaling measure [1]. However, in some structures, due to geometrical complexity, several fractal structures overlap simultaneously and are considered as multifractal objects [2]. These multifractal objects are completely characterised by a function, known as a generalised dimensions function ($D(q)$) [3]. The box-counting method and the method of moments [4] allow to carry out a simple and robust multifractal analysis on images. These methods are able to estimate the generalised fractal dimensions, $D(q)$, and describe complex structures with sets of regions exhibiting different fractal properties, providing a relatively more concrete characterisation.

From a fractal approach, image analysis is typically accomplished on binary [5] or RGB images [6] [7]; however, they

are hardly found from a multifractal approach nor in different colour formats [8] [9]. For this reason, a novel methodology for analysing images in different colour formats by means of multifractal analysis is proposed in this work. Specifically, four well-known formats namely RGB, CMYK, HSV and HSI, are analysed and compared using the multifractal box-counting method. The analysis has been carried out on thermal images of a Pi3 Raspbian Desktop board, in order to make a first approach towards the characterisation of electronic devices based on heat dissipation. Additionally, three different areas of the board are analysed, in order to provide our study with different cases of study. Results show that the multifractal analysis varies depending on the colour profile, i.e., the same image, depending on the colour format, presents different multifractal properties. This result points out that the image colour profile may hinder the multifractal properties of the heat dissipation of the electronic device. Therefore, it is concluded that in order to carry out a multifractal analysis of thermal images, the raw file should ideally be considered to avoid alterations in the results.

The paper is organised as follows. Section II briefly presents the most relevant works in the state of the art. Section III introduces the methodology proposed in this work. Thermal image acquisition and multifractal analysis are described in sections III-A and III-B, respectively. Results are explained in Section IV. Finally, Section V concludes the work.

II. RELATED WORKS

Fractal analysis has extensively been used for the analysis of digital images [5], however, there are few studies of digital colour images using a more comprehensive approach, the multifractal analysis. Most of the existing fractal methods for analysing images are defined for 1D signal or binary images, extending to Grey-Scale images [5]. In [8], a multifractal analysis using the box-counting method is applied on RGB images. Specifically, the authors analyse a three-dimensional histogram of the image, which contains the R, G and B colour coordinates. In the same way, in [10] the three-dimensional

histogram of RGB images is also analysed. However, here, the authors use the multifractal analysis as an image noise detection tool. In works such as [9], RGB images are analysed by decomposing the channels that make up each image. They propose a methodology similar to the one proposed in this work. However, they only select one channel from the RGB image and then binarise it, so the multifractal analysis is actually conducted on binary images, unlike the proposed work, where the pixels of the analysed images take values from 0 to 255. Furthermore, in this work, not only are RGB images analysed, but also images in different colour formats (including all the channels that compose each format). Moreover, [6] highlights the difficulty in estimating the fractal dimension of RGB colour images. Finally, [7] again analyses RGB and Grey-Scale images from a fractal approach using the box-counting method. The authors adopt a methodology similar to the one followed in this work, since they analyse a Grey-Scale image as well as each of the channels that make up the RGB image.

As it can be seen, the number of existing studies on images considering different colour formats from a multifractal approach is low. For this reason, the purpose of this work is to present a new methodology, using multifractal analysis, to characterise images in different colour formats, in order to evaluate the influence of the colour format in the results of the analysis. Specifically, this work is focused on analysing thermal images of an electronic device with the aim of establishing robust relationships between the multifractal characteristics of the device and heat dissipation in the future.

III. METHODOLOGY

This section is structured in two subsections. Section III-A summarises the thermal images under study, as well as the image capture process and image processing. Then, the multifractal analysis approach and its application to the study of thermal images is explained in Section III-B.

A. Thermal images

The images under study correspond to a Pi3 Raspbian Desktop board, on which the basal consumption was evaluated. That is, the images are captured during the base consumption of the Operating System, from an initial state, when the board is turned off, to a second state, after one hour, when the board is on. It should be noted that the images were taken by the authors. The images in the different colour profiles have also been created by them.

The image capture is performed by a FLIR ETS320 infrared camera, which allows the visualisation of hot spots and potential failure points, capturing the emissivity of the object. This camera model has a wide temperature range $[-20^{\circ}\text{C}, 250^{\circ}\text{C}]$ with a measurement accuracy of $\pm 3^{\circ}\text{C}$, allowing to quantify the heat generation and heat dissipation of small components (up to $170\ \mu\text{m}$). It consist of an InfraRed (IR) Sensor, which offers 76,800 points of non-contact temperature measurement. Finally, standard radiometric jpeg files are obtained, with 14 bit measurement data.

Image capture is carried out for one hour (3,600 seconds), from an initial time ($t_0 = 0\text{s}$) when the board is off, to a second time ($t_1 = 3,600\text{s}$), so the board is on for an hour. During this time period, a total of 31,970 images of the board were captured, at an average of 8-9 images per second. This camera model produces rectangular images of 320×240 pixels. In Figure 1, an example of the captured images is shown.



Figure 1. Example of a 320×240 pixel image of the board.

The subsequent method used for multifractal analysis requires that the analysed images must be square with a side length power of 2. For this, each of the rectangular images on the board is cropped into different square sub-images of 128×128 pixels. Specifically, this study focuses on three different areas of the board at three different time instants. In this way, three 128×128 pixels square cutouts were obtained, each one corresponding to a different time instant, which are independent of each other (see Figure 2). It should be noted that each of the images in Figure 2 will be studied, from a multifractal approach, in different colour profiles: Grey-Scale (GS), RGB, CMYK, HSV and HSI (see Figure 3).

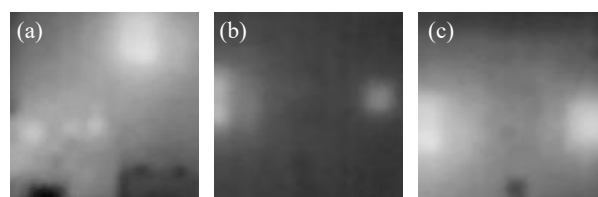


Figure 2. Images of different areas of the board at different time instants, (a) Image area 1, (b) Image area 2, (c) Image area 3.

As already mentioned, the images obtained by the infrared camera represent the emissivity values captured by the IR sensor (values from 0.0 to 1.0). Subsequently, a normalisation is carried out, where these values between 0 and 1 become the values of a Grey-Scale image (values between 0 and 255). These Grey-Scale images are used as a reference, because they are considered to represent the most faithful and realistic situation to the raw files captured by the camera.

B. Multifractal Analysis

Fractal shapes are mainly characterised by the fact that the measurement of the object is dependent on the scale of measurement. When this dependence follows a power law, it

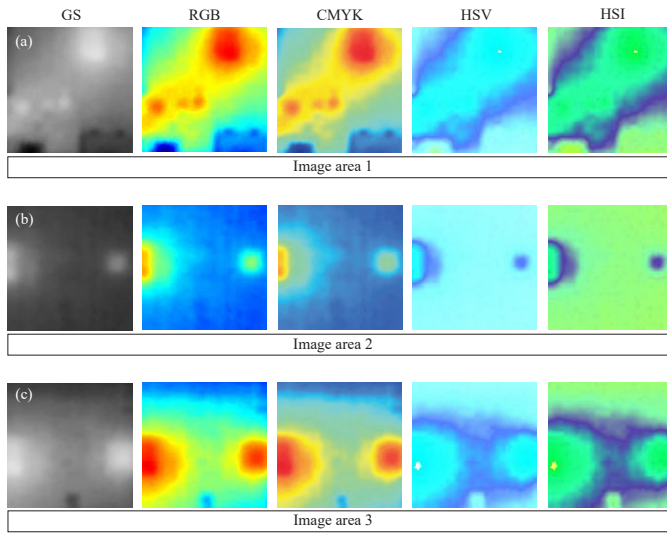


Figure 3. Images corresponding to the three defined areas of the board in each of the four different colour profiles: RGB, CMYK, HSK, HSI, and the Grey-Scale image (GS).

is said that the object manifests fractal properties. The main parameter is known as the fractal dimension (D_f), which is estimated by means of the slope of the linear fit on the log-log relationship between the scale and the measure [11] [12]. However, due to geometrical complexity, several fractal structures overlap simultaneously and are considered as multifractal objects. Multifractal objects are completely characterised by a function, known as a generalised dimensions function, $D(q)$ [13] [14]. The main advantage of multifractal analysis is the description of complex structures exhibiting sets of regions with different fractal properties, providing a relatively more specific characterisation [2].

To carry out the multifractal analysis, it is proposed to use the box-counting method along with the method of moments [4]. These methods allow a robust estimation of the generalised fractal dimensions, $D(q)$ [13] [14]. In the box-counting method, an image of side L is completely covered by a set of square boxes, of side δ , which do not overlap. Values of δ are obtained as follows: $\delta = \{L/1, L/2, L/4, L/8, \dots\}$. Regarding the method of moments, parameter q is a remarkable one, which is a real value varying between $-\infty$ and $+\infty$ [2]. Positive q values magnify regions with high colour intensity values, while negative q values intensify regions with low colour intensity values. With these methods, the partition function, $\chi(q, \delta) = \sum_{i=1}^n (c_i(\delta))^q$, is obtained, being $(c_i(\delta))^q$ the mass probability function. It is well known that multifractality appears when the existence of a power law between $\chi(q, \delta)$ vs. δ is trusted. This function allows to differentiate the scale ranges (δ) where the linear fits will be performed. In this work, it is taken as a criterion to select the scale range where all the moments q can be considered, both positive and negative, and where, in addition, there is linearity. Once the range of scales is established, we turn to the generalised dimensions function, $D(q) = \frac{\tau(q)}{q-1}$, where $\tau(q)$ is the mass exponent function. $\tau(q)$

is obtained from the slope of the linear fittings performed in the selected regions of the partition function.

Notice that $D(q)$ exhibits multifractal behaviour when it is a monotonically decreasing function dependent on q . By contrast, it is considered monofractal when $D(q)$ is independent of q , i.e., it is represented by a horizontal straight line of constant slope. Another multifractal parameter used in this work is the degree of multifractality, $\Delta D(q) = D(q_{min}) - D(q_{max})$. This parameter indicates the multifractal strength of the image, i.e., the higher the $\Delta D(q)$ value, the greater the multifractality of the image. By contrast, the smaller the $\Delta D(q)$ value, the more monofractal it is.

In this work, we first propose to study the partition functions of each image establishing the scale ranges where the linear fits will be made to complete the analysis. Note that there will be a partition function for each of the channels that make up each colour profile. Subsequently, once the scale ranges have been established, the values of $D(q)$ are computed and depicted against q to obtain the generalised dimensions function. Finally, since Grey-Scale images are considered as reference images, comparisons are made with the different colour formats. For this purpose, the difference between the values of the Grey-Scale dimension functions and the dimension functions of each channel is evaluated. This difference allows to determine the channels and scale ranges that capture the multifractal behaviour of the original image and, therefore, determine which colour format and/or channel is more representative of each original image.

IV. RESULTS AND DISCUSSION

In this section, the main findings after applying the box-counting and the method of moments to the image set are shown. First, the results of the analysis of the image of reference, i.e., the Grey-Scale, are presented followed by the RGB, CMYK, HSV and HSI formats. Finally, a comparison between the colour formats and the Grey-Scale images is accomplished.

A. Multifractal Analysis of Grey-Scale images

First of all, it should be noted that the box-counting method and the method of moments are used to carry out the multifractal analysis. Both are performed in Matlab software. In this case, for an image size of 128x128 pixels, the values of the scale (δ) range from $\delta = 2^0 = 1$ to $\delta = 2^7 = 128$. The values of the moments q are set between -4 and 4.

The partition functions of the three images selected and represented in Grey-Scale (see Figure 2) present similar shapes. Figure 4 (a) shows the partition function corresponding to the image of the area 1 of the board. However, it is representative of the rest of the Grey-Scale images. As observed, none of them show crossovers that distinguish scale ranges, i.e., a single linear region is observed from $\delta = 1$ to $\delta = 128$. In this way, the generalised dimensions function, $D(q)$, can be completely reconstructed for all moments q . Linear fits are performed with a coefficient R^2 greater than 0.99 for all cases. Figure 4 (b) shows the generalised dimensions function, $D(q)$,

corresponding to the image of the area 1 of the board. Again, it is representative of the rest of the Grey-Scale images. As seen, the generalised dimension function is horizontal, thus it can be considered as a monofractal behaviour.

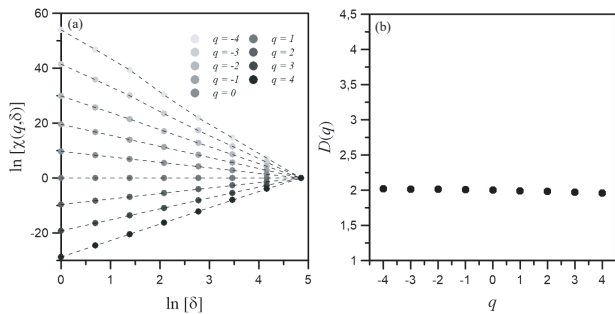


Figure 4. Graphs corresponding to the image of the area 1, (a) Partition function, (b) Generalised dimensions function.

Table I shows the results for the $D(q)$ of the three areas of the board. The values of $D(q)$ exhibit a very small degree of multifractality, so that, monofractal behaviour is considered in all three cases. It should be noted that the $\Delta D(q)$ of image area 1 is higher than in the rest of the images. This is due to the fact that the estimation for negative q values is worse. However, the rest of the function $D(q)$ is monofractal. Images of areas 2 and 3 are completely monofractal.

TABLE I. MULTIFRACTAL PARAMETERS OF THE 3 GREY-SCALE IMAGES

Degree of multifractality, $\Delta D(q)$	Image area 1	0.279
	Image area 2	0.059
	Image area 3	0.074

B. Multifractal Analysis of RGB images

In Figure 5, the partition functions obtained from the image of area 1 of the board for the 3 channels of the RGB colour profile are shown, as an example. In contrast to Grey-Scale images, the RGB images have different crossovers depending on the colour channel, so that there are different linear regions. Therefore, multifractal analysis is performed in different scale ranges depending on the colour channel. The same behaviour is observed for the RGB images of areas 2 and 3, i.e., depending on the image and the colour channel, partition functions with linear regions differing from each other are obtained.

Table II summarises the results obtained from the 3 RGB images analysed. On the one hand, the values of the degree of multifractality, $\Delta D(q)$, are presented. On the other hand, in order to detect which channel is capable of exhibiting the same monofractal behaviour as the reference Grey-Scale image (see Table I), the quadratic error ($\sum x^2 = \sum (D(q)_{gs} - D(q)_c)^2$) is estimated, which summarises the differences between the Grey-Scale and the colour channel. A value of the difference less than or equal to 0.2 is considered acceptable.

It should be noted that Table II indicates which colour channels do or do not exhibit scaling behaviour for a given range

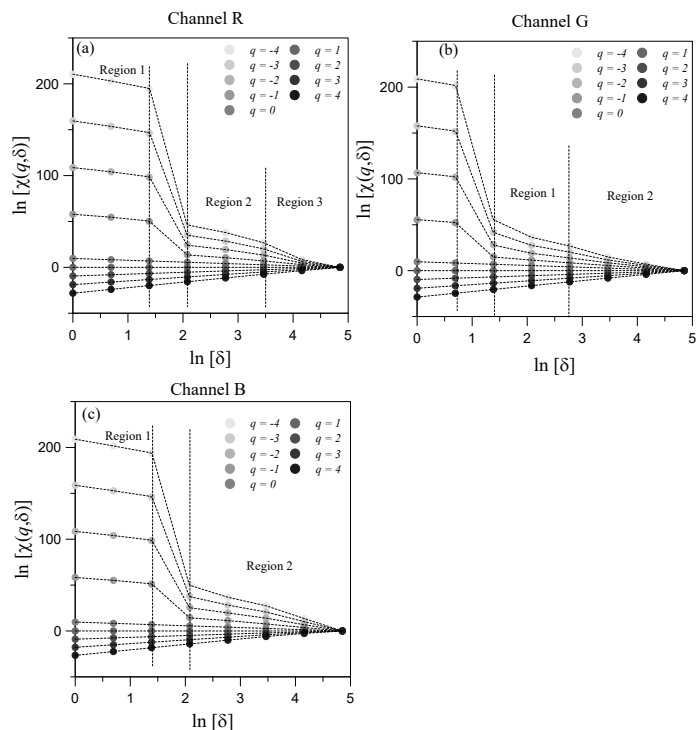


Figure 5. Partition functions of the RGB image of area 1, (a) Partition function of channel R, (b) Partition function of channel G, (c) Partition function of channel B. The crossovers for the linear fits have been made by vertical broken lines.

of scales. That is, scaling behaviour exists when the values of $D(q)$ are constant (monofractal) or decrease (multifractal) as the q moments grow. Increasing $D(q)$ functions implies a non-scaling behaviour. Therefore, regions which exhibit scaling behaviour are denoted by the symbol \checkmark , otherwise they are marked with $-$. In Table II, Scaling Behaviour is denoted as SB.

As it can be seen in Table II, only channel G presents a scaling behaviour in all the δ regions for the three images. For channel R, only one δ region of images 1 and 2 show scaling properties, as opposed to channel B, where only one δ region of images 1 and 3 do not show it. In terms of the $\sum x^2$, regions exhibiting the least difference compared to the Grey-Scale images are specified next: In G channel, region 2 ($\delta = 16 - 128$) for the image of area 1; region 1 ($\delta = 1 - 128$) for the image of area 2; and region 2 ($\delta = 16 - 128$) for the image of area 3. In channel B, only in the image of area 2, specifically in the region 2 ($\delta = 16 - 128$). In channel R, an adequate approximation to the multifractal behaviour of the Grey-Scale reference image is not achieved.

C. Multifractal Analysis of CMYK images

The partition functions of the CMYK image 1 area 1 are shown in Figure 6 as a representative example. As seen, the CMYK images also show different partition functions depending on the chosen colour channel. Each of the channels that make up the CMYK colour profile have different linear

TABLE II. MULTIFRACTAL PARAMETERS OF THE 3 RGB IMAGES. COMPARISON WITH THE GREY-SCALE REFERENCE IMAGES

Channel R		SB ^a	$\Delta D(q)$	$\sum x^2$
$\Delta D(q)$ Image 1	Reg. 1 $\delta = 1 - 4$	-	-	-
	Reg. 2 $\delta = 8 - 32$	-	-	-
	Reg. 3 $\delta = 32 - 128$	✓	2.051	6.363
$\Delta D(q)$ Image 2	Reg. 1 $\delta = 1 - 8$	-	-	-
	Reg. 2 $\delta = 16 - 128$	✓	2.400	8.150
$\Delta D(q)$ Image 3	Reg. 1 $\delta = 1 - 4$	-	-	-
	Reg. 2 $\delta = 8 - 32$	-	-	-
Channel G		SB ^a	$\Delta D(q)$	$\sum x^2$
$\Delta D(q)$ Image 1	Reg. 1 $\delta = 4 - 16$	✓	2.224	9.179
	Reg. 2 $\delta = 16 - 128$	✓	0.588	0.165
$\Delta D(q)$ Image 2	Reg. 1 $\delta = 1 - 128$	✓	0.072	0.001
$\Delta D(q)$ Image 3	Reg. 1 $\delta = 4 - 16$	✓	3.112	21.062
	Reg. 2 $\delta = 16 - 128$	✓	0.436	0.186
Channel B		SB ^a	$\Delta D(q)$	$\sum x^2$
$\Delta D(q)$ Image 1	Reg. 1 $\delta = 1 - 4$	-	-	-
	Reg. 2 $\delta = 8 - 128$	✓	1.862	4.937
$\Delta D(q)$ Image 2	Reg. 1 $\delta = 4 - 16$	✓	1.980	8.251
	Reg. 2 $\delta = 16 - 128$	✓	0.315	0.116
$\Delta D(q)$ Image 3	Reg. 1 $\delta = 1 - 4$	-	-	-
	Reg. 2 $\delta = 8 - 32$	✓	0.622	0.774

^a SB: Scaling Behaviour

regions between them, so the multifractal analysis is performed in different scale ranges and, therefore, different results are obtained for each channel.

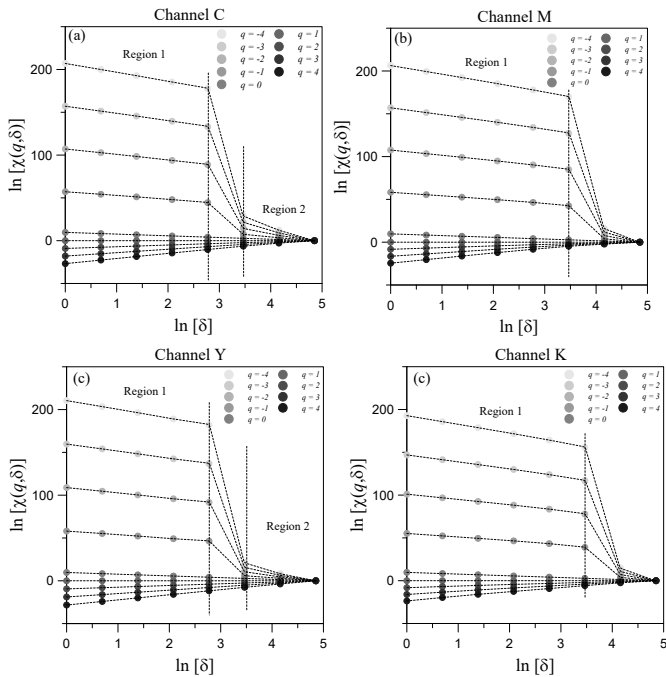


Figure 6. Partition functions of the CMYK image area 1, (a) Partition function of channel C, (b) Partition function of channel M, (c) Partition function of channel Y, (d) Partition function of channel K.

The same procedure used in the analysis of RGB images is explained next. First, it is determined which channel exhibits a scaling behaviour. In this case, with respect to channel C, the

image of area 1 in region 2 ($\delta = 32 - 128$) shows a scaling behaviour, as well as the image of area 2 for the regions 1 ($\delta = 1 - 8$) and 2 ($\delta = 16 - 128$). On the other hand, no scaling features are found in the image area 3. In terms of channel M, only region 2 ($\delta = 32 - 128$) of the image of area 2 shows a scaling behaviour. In channel Y, both images 1 and 2, both in region 2 ($\delta = 32 - 128$), present scaling properties. Finally, in channel K, only the region 2 of image of area 2 ($\delta = 32 - 128$) exhibits a scaling behaviour.

Once the scale ranges where a scaling behaviour occurs have been established, a comparison with the Grey-Scale images is made. Only channel C can capture the scaling behaviour of the reference image, specifically in image area 2 for both scale ranges. In this case, it could be considered that the CMYK colour profile does not provide proper results, since it fails to capture the monofractality of the original image.

D. Multifractal Analysis of HSV images

The HSV images present the same behaviour as the previous ones, i.e., each of the images analysed shows different partition functions depending on the channel. In Figure 7, the partition functions of the HSV image area 1 are shown as a representative example. Again, as it can be seen, different linear regions and different scale ranges are obtained from the multifractal analysis.

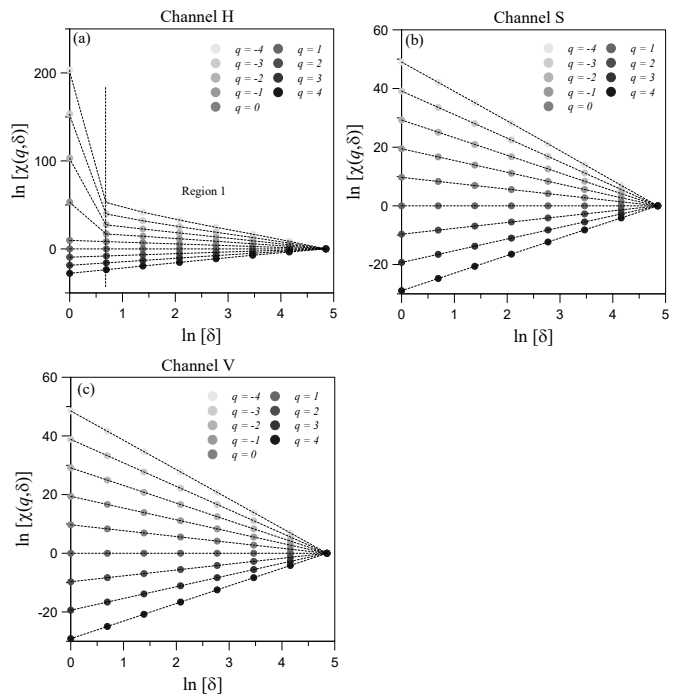


Figure 7. Partition functions of the HSV image area 1, (a) Partition function of channel H, (b) Partition function of channel S, (c) Partition function of channel V.

Next, the scale ranges that exhibit a scaling behaviour are explained. Regarding channel H, the 3 analysed images present scaling features in region 1, specifically from $\delta = 2$ to $\delta = 128$ for the image of areas 1 and 3, and from $\delta = 1$ to $\delta = 128$

for image area 2. The same result is found for channels S and V, where the images exhibit scaling properties for region 1 ($\delta = 1$ to $\delta = 128$).

In terms of the comparison with the Grey-Scale reference images, it is noteworthy to mention that all 3 channels are capable of capturing the scaling behaviour of the reference images, except in the case of image area 3 and channel H.

E. Multifractal Analysis of HSI images

Finally, the results obtained in the analysis of the HSI images are discussed. Again, for the same image, each colour channel has different linear regions (see Figure 8). This happens in the rest of images, as already discussed in the previous cases.

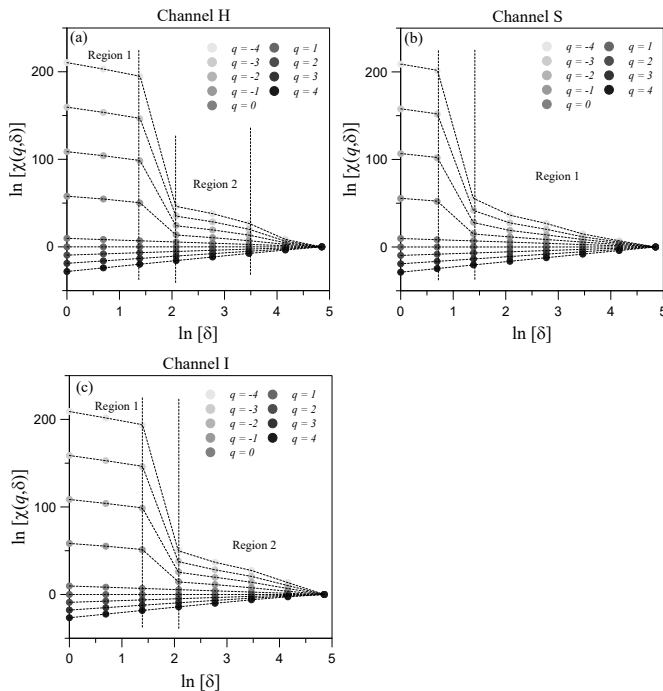


Figure 8. Partition functions of the HSI image area 1, (a) Partition function of channel H, (b) Partition function of channel S, (c) Partition function of channel I.

The scale ranges that exhibit a scaling behaviour are explained next: In channel H, the image of area 1 for a scale range from $\delta = 8$ to $\delta = 32$ in region 2, as well as image area 2 for the region 2 ($\delta = 16 - 128$), and image area 3 again in region 2 ($\delta = 8 - 32$). In channel S, a scaling behaviour is found in region 1 ($\delta = 4 - 128$) of the image of area 1, in the image of area 2 in region 1 ($\delta = 1 - 128$) and in the image of area 3 in regions 1 ($\delta = 4 - 16$) and 2 ($\delta = 16 - 128$). In I channel, image area 1 shows scaling features in region 2 ($\delta = 8 - 128$), the image area 2 in regions 1 ($\delta = 4 - 16$) and 2 ($\delta = 16 - 128$), and image of area 3 only in region 2 ($\delta = 8 - 32$).

Compared to the Grey-Scale reference images, it should be highlighted that channel H fails to capture the reference scaling behaviour in any of the images. Regarding channel

S, the results are acceptable for the image of area 2, in region 1 ($\delta = 1 - 128$), and in image of area 3 in region 2 ($\delta = 16 - 128$). Finally, channel I only provides acceptable results for image area 2, specifically in region 2 ($\delta = 16 - 128$).

F. Comparison between Grey-Scale images and colour formats

The aim of this subsection is to summarise the colour channels that have been detected as the best approximation to the monofractal behaviour of the Grey-Scale reference images. In order to do so, the focus is on the difference between the $D(q)$ values of the Grey-Scale images and those of the colour models assessed with the quadratic error ($\sum x^2$). Table III shows how the colour channels resemble to the original image measured as percentage. This percentage is calculated by considering the colour channels that exhibit scaling behaviour and taking into account those whose quadratic error ($\sum x^2$) is less than or equal to 0.2. This way, those colour channels that have presented a lower error will have a higher percentage. That is, if a channel, in all cases, has managed to capture the monofractal behaviour of the reference image, it will have a percentage of 100% and, therefore, if it has not been able to capture such behaviour in any of the cases, it will be scored with 0%. Therefore, the higher the percentage value, the more representative and better approximation the channel presents. It should be noted that Table III shows the results of the three images analysed from an overall global approach.

TABLE III. APPROXIMATION BETWEEN GREY-SCALE REFERENCE IMAGES AND DIFFERENT COLOUR PROFILES IN PERCENTAGE

Colour profile		Approximation rate (%)
RGB	Channel R	0%
	Channel G	60%
	Channel B	25%
CMYK	Channel C	67%
	Channel M	0%
	Channel Y	0%
	Channel K	0%
HSV	Channel H	67%
	Channel S	100%
	Channel V	100%
HSI	Channel H	0%
	Channel S	50%
	Channel I	25%

As seen, three out of the four colour formats studied fail to capture the reference monofractal behaviour. For RGB, CMYK and HSI formats, there is at least one channel that can not be accepted as a proper approximation of the reference images, exhibiting a percentage of 0%. By contrast, there are other channels with an acceptable approximation with a percentage over 60%, e.g., channels G, C and S for RGB, CMYK and HSI, respectively. Finally, the HSV colour model provides proper results, since a high approximation (between 67% and 100%) is achieved for three channels and their three images.

V. CONCLUSIONS

This work proposes a novel methodology to analyse images in different colour formats: Grey-Scale, RGB, CMYK, HSV

and HSI by means of a multifractal approach based on the box-counting method and the method of moments. The study is carried out on thermal images of a Raspberry Pi3 electronic device.

Results show that the images in all the studied colour profiles have different partition functions as well as different scale ranges. This implies that the multifractal analysis varies depending on both the image format and the colour profile. In fact, the same image presents different multifractal behaviour depending on the colour format. On the contrary, the partition functions of the Grey-Scale images show linearity for all values of δ (1-128) in all images analysed.

The capability of capturing the behaviour of the original image of each format is evaluated by estimating the approximation of each colour channel with respect to the Grey-Scale image.

Results show that the CMYK colour profile is not considered suitable, as it fails to capture the multifractal behaviour of the original image in most of its channels. Among them some channels of RGB and HSI are able to approximate to the behaviour of the original image, the HSV arises as the most suitable format for analysing thermal images from a multifractal approach. Finally, it should also be noted that the capability to reproduce the monofractal behaviour of Grey-Scale images also depends on the range of scales considered (δ). For RGB and HSI formats, the scale range is usually from 16 to 128, so no monofractality can be found for scales ($\delta < 16$). Conversely, in the HSV format, the scale range covers the entire image with δ ranging from 1 to 128, so in this sense, this format is the one that exhibits monofractality over a larger range of scales.

The disparity of scaling behaviours found for different image channels and formats suggests an in-depth study on the multifractal features of images represented in different formats using the usual image analysis benchmarks from the literature is needed. As future work, it would be interesting to build a meta-model, in which different formats would consider their “understanding” of the image, while that meta-model would combine their “opinions”.

ACKNOWLEDGMENT

Work supported by eFracWare project (TED2021-131880B-I00), funded by Spanish MCIN and the European Union “NextGenerationEU”/PRTR on MCIN/AEI/10.13039/501100011033, and eMob (PID2022-137858OB-I00), funded by Spanish MCIN/AEI/10.13039/501100011033/FEDER, UE.

REFERENCES

- [1] B. Mandelbrot, “How long is the coast of Britain? statistical self-similarity and fractional dimension,” *Science*, vol. 156, pp. 636–638, 1967.
- [2] A. N. Kravchenko, C. W. Boast, and D. G. Bullock, “Multifractal analysis of soil spatial variability,” *Agronomy Journal*, vol. 91, no. 6, pp. 1033–1041, 1999.
- [3] M. S. Jouini, S. Vega, and E. A. Mokhtar, “Multiscale characterization of pore spaces using multifractals analysis of scanning electronic microscopy images of carbonates,” *Nonlinear Processes in Geophysics*, vol. 18, pp. 941–953, 2011.
- [4] C. Evertsz and B. Mandelbrot, “Appendix b. multifractal measures. chaos fractals,” *Springer*, pp. 922–953, 1992.
- [5] M. Ivanovici and N. Richard, “Fractal dimension of color fractal images,” *IEEE Trans. Image Processing*, vol. 20, pp. 227–235, 1 2011.
- [6] S. R. Nayak, J. Mishra, A. Khandual, and G. Palai, “Fractal dimension of rgb color images,” *Optik*, vol. 162, pp. 196–205, 6 2018.
- [7] S. Verdú, J. Barat, and R. Grau, “Fresh-sliced tissue inspection: Characterization of pork and salmon composition based on fractal analytics,” *Food and Bioproducts Processing*, vol. 116, pp. 20–29, 7 2019.
- [8] J. Chauveau, D. Rousseau, P. Richard, and F. Chapeau-Blondeau, “Multifractal analysis of three-dimensional histogram from color images,” *Chaos, Solitons and Fractals*, vol. 43, pp. 57–67, 2010.
- [9] N. Reljin, M. Slavkovic-Ilic, C. Tapia, N. Cihoric, and S. Stankovic, “Multifractal-based nuclei segmentation in fish images,” *Biomedical Microdevices*, vol. 19, no. 17, 9 2017.
- [10] R. Uthayakumar and D. Easwaramoorthy, “Multifractal analysis in denoising of color images,” *IEEE*, 2012, pp. 228–234.
- [11] B. Mandelbrot, *The fractal geometry of nature*, 3rd ed. New York: W. H. Freeman and Comp., 1983.
- [12] J. Feder, *Fractals*, ser. Physics of Solids and Liquids. Springer, 2013.
- [13] P. Grassberger, “Generalized dimensions of strange attractors,” *Phys. Lett. A*, vol. 97, no. 6, pp. 227–230, 1983.
- [14] H. Hentschel and I. Procaccia, “The infinite number of generalized dimensions of fractals and strange attractors,” *Physica 8D*, vol. 8, pp. 435–444, 1983.